Articles

An Examination of the Role of Asp-177 in the His-Asp Catalytic Dyad of *Leuconostoc mesenteroides* Glucose 6-Phosphate Dehydrogenase: X-ray Structure and pH Dependence of Kinetic Parameters of the D177N Mutant Enzyme[†,‡]

Michael S. Cosgrove,[§,⊥] Sheila Gover,[∥] Claire E. Naylor,[∥] Lucy Vandeputte-Rutten,[∥] Margaret J. Adams,[∥] and H. Richard Levy*[,§]

Department of Biology, Syracuse University, Syracuse, New York 13244, and Laboratory of Molecular Biophysics, Department of Biochemistry, University of Oxford, Oxford OX1 3QU, United Kingdom

Received June 27, 2000; Revised Manuscript Received September 25, 2000

ABSTRACT: The role of Asp-177 in the His-Asp catalytic dyad of glucose 6-phosphate dehydrogenase from *Leuconostoc mesenteroides* has been investigated by a structural and functional characterization of the D177N mutant enzyme. Its three-dimensional structure has been determined by X-ray cryocrystallography in the presence of NAD^+ and in the presence of glucose 6-phosphate plus NADPH. The structure of a glucose 6-phosphate complex of a mutant (Q365C) with normal enzyme activity has also been determined and substrate binding compared. To understand the effect of Asp-177 on the ionization properties of the catalytic base His-240, the pH dependence of kinetic parameters has been determined for the D177N mutant and compared to that of the wild-type enzyme. The structures give details of glucose 6-phosphate binding and show that replacement of the Asp-177 of the catalytic dyad with asparagine does not affect the overall structure of glucose 6-phosphate dehydrogenase. Additionally, the evidence suggests that the productive tautomer of His-240 in the D177N mutant enzyme is stabilized by a hydrogen bond with Asn-177; hence, the mutation does not affect tautomer stabilization. We conclude, therefore, that the absence of a negatively charged aspartate at 177 accounts for the decrease in catalytic activity at pH 7.8. Structural analysis suggests that the pH dependence of the kinetic parameters of D177N glucose 6-phosphate dehydrogenase results from an ionized water molecule replacing the missing negative charge of the mutated Asp-177 at high pH. Glucose 6-phosphate binding orders and orients His-178 in the D177N−glucose 6-phosphate−NADPH ternary complex and appears to be necessary to form this water-binding site.

Glucose 6-phosphate dehydrogenase (G6PD, EC 1.1.1.49)[1] from *Leuconostoc mesenteroides* catalyzes the oxidation of glucose 6-phosphate (G6P) using $NADP^+$ or NAD^+. The enzyme has been cloned and expressed in *Escherichia coli* (*1*), and its three-dimensional structure in the presence of bound inorganic phosphate, a substrate inhibitor, has been determined by X-ray crystallography (*2*). The 2 Å resolution structure of G6PD led to the proposal that His-240 is the general base that abstracts a proton from the C1 hydroxyl group of G6P, allowing transfer of the C1 hydride to the nicotinamide ring of the coenzyme. The Nϵ2 of His-240 is optimally positioned for proton abstraction relative to the putative substrate-binding site, while its Nδ1 is hydrogen-bonded to the Oδ1 of Asp-177 (Scheme 1). The roles of His-240 and Asp-177 in catalysis have been examined previously by site-directed mutagenesis of each to asparagine (*3*). The results of these studies and chemical modification studies (*4*−*6*) support the proposal that His-240 is the general base catalyst. Asp-177 was proposed to participate in catalysis by stabilizing the positive charge that forms on His-240 in the transition state, thus forming a catalytic dyad (*3*).

The function of the aspartate in various His-Asp catalytic dyads has been the subject of much study and debate. It has been postulated that the aspartate functions by (i) orienting the imidazole ring of the histidine to optimize the geometry for proton abstraction, (ii) modulating the pK_a of the histidine

[†] Supported by Grant MCB-9513814 from the National Science Foundation.

[‡] The atomic coordinates for the D177N enzyme grown with NAD^+ (1e7m) and with G6P plus NADPH (1e7y) and those for the Q365C enzyme with G6P (1e77) have been deposited with the Protein Data Bank.

* Corresponding author. Phone: 315-443-3181. Fax: 315-443-2012. E-mail: hrlevy@mailbox.syr.edu.

[§] Syracuse University.

[∥] University of Oxford.

[⊥] Current address: Department of Biophysics and Biophysical Chemistry, Johns Hopkins School of Medicine, 725 North Wolfe Street, Baltimore, Maryland 21205.

[1] Abbreviations: G6PD, glucose 6-phosphate dehydrogenase; G6P, glucose 6-phosphate; PAGE, polyacrylamide gel electrophoresis; SDS, sodium dodecyl sulfate; MES, 2-(*N*-morpholino)ethanesulfonic acid; PIPES, piperazine-*N*,*N*′-bis(2-ethanesulfonic acid); HEPES, *N*-2-hydroxyethylpiperazine-*N*′-2-ethanesulfonic acid; Tris, tris(hydroxymethyl)aminomethane; CHES, cylcohexylaminoethane-sulfonic acid; CAPS, 3-(cyclohexylamino)-propanesulfonic acid; BAD, benzamide adenine dinucleotide.

10.1021/bi0014608 CCC: $19.00
Published on Web 11/14/2000

Scheme 1 : Proposed Catalytic Mechanism for the Reaction Catalyzed by G6PD (*3*)

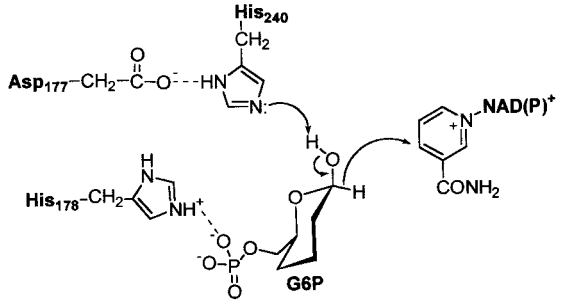

to improve the basicity/acidity during the course of the reaction, and/or (iii) keeping histidine in the proper tautomeric form. Studies that distinguish among these possibilities have utilized site-directed mutagenesis to replace aspartate with asparagine or alanine and to assess the structural and functional characteristics of the mutated enzymes. Using this approach with rat trypsin, Sprang et al. (*7*) suggested that the function of Asp-102 (chymotrypsin numbering) of the Asp-His-Ser catalytic triad was to stabilize the productive tautomer of the catalytic His-57. A similar role was indicated for Asp-121 of the His-Asp catalytic dyad of ribonuclease A (*8*), suggesting this function may be general. In contrast, structural and functional studies on the D270N mutant of mandelate racemase suggest that Asp-270 prevents the depression of the pK_a of the *R*-specific acid/base catalyst, His-297, from the positive electrostatic potential of the active site (*9*). This result suggests that the aspartate in the His-Asp catalytic dyad may also be important in orienting the catalytic base and affecting its pK_a. To elucidate the function of the aspartate in G6PD, we have replaced Asp-177 with asparagine by site-directed mutagenesis and analyzed the structural and functional properties of the D177N enzyme.

The steady state kinetic parameters of D177N G6PD at pH 7.8 were reported previously (*3*). The k_{cat} for the reaction is 2 orders of magnitude lower than that for the wild-type enzyme in both the NAD- and NADP-linked reactions with little effect on Michaelis constants for substrate and coenzyme and only a 9-fold increase in the K_m for NAD^+. We concluded that Asp-177 is important for the catalytic mechanism by making His-240 a better general base (*3*). To test this hypothesis, the structural and functional characteristics of D177N G6PD have been examined further. Three-dimensional structures have been determined by X-ray cryocrystallography of the D177N mutant enzyme, in the presence of NAD^+ and in the presence of G6P plus NADPH, and of the G6P complex of the mutant Q365C−G6PD, which has normal enzymatic activity. These structures are compared in order to determine if Asp-177 in wild-type G6PD is required to orient His-240 or if it is also necessary to stabilize its proper tautomeric form. To understand the effect of Asp-177 on the ionization properties of His-240, the pH dependence of kinetic parameters has been determined for D177N G6PD and is compared to that of wild-type G6PD.

MATERIALS AND METHODS

Materials. Coenzymes were obtained from Boehringer Mannheim; Matrex gel Purple A, Matrex gel Orange B, and CF-50 Centriflo membrane cones were obtained from Amicon Corp.; G6P was obtained from Sigma; Coomassie protein assay reagent and bovine serum albumin standard were obtained from Pierce; Sequenase version 2.0 DNA sequencing system and Sculptor in vitro mutagenesis system were obtained from Amersham International plc; Prep-A-Gene DNA purification system was obtained from Bio-Rad; pUC-19, M-13 bacteriophage, T4 polynucleotide kinase, and DNA ligase were obtained from Gibco-BRL; restriction endonucleases were obtained from New England Biolabs. The oligonucleotide for site-directed mutagenesis was synthesized by Ransom Hill Bioscience Inc. The oligonucleotide sequence of D177N was as follows (change from the wild-type sequence in boldface): TTCCGTATT**A**ACCACTAC

Site-Directed Mutagenesis. All standard DNA techniques were performed as described by Sambrook et al. (*10*) and as previously reported (*11*). Site-directed mutagenesis was performed with the Amersham in vitro mutagenesis system, using the oligonucleotide listed above. Mutations were constructed in M-13 bacteriophage, subcloned into pUC19, and transformed into *E. coli* strain SU294, which lacks the G6PD gene (*12*). Plasmids were isolated, and the entire G6PD gene was sequenced to ensure that no other mutations were introduced.

Purification and Assay of G6PD Activity. Recombinantly expressed wild-type and D177N G6PDs were purified to homogeneity (data not shown) by the methods described previously (*12*). Recombinant Q365C−G6PD was purified as described previously (*13*). Routine assays for G6PD activity were performed at 25 °C in a Gilford 240 spectrophotometer at 340 nm by following the rate of appearance of NADPH. Assays were initiated by the addition of enzyme to 1.0 mL of 33 mM Tris-HCl, pH 7.8, containing 2.28 mM G6P and 0.160 mM $NADP^+$. Protein concentrations were determined from the extinction coefficient of wild-type G6PD at 280.5 nm (*14*).

pH Dependence of Kinetic Parameters. The dependence of the kinetic parameters on pH was determined as described by Viola (*15*). This involved determining k_{cat} and k_{cat}/K_m values for wild-type and D177N G6PDs over the pH range from 4.0 to 11.0 at 25 °C. The buffers sodium acetate, MES, PIPES, HEPES, CHES, and CAPS were used within ±1 pH unit of their pK_a values. Overlapping pH ranges were used to ensure that any discontinuities would be detected. Ionic strength was maintained at 0.1 M by the addition of sodium acetate. Acetate was shown not to affect the activity of G6PD. The pH of reaction mixtures was measured before and after the reaction and never deviated more than ±0.1 pH units from the pH of the buffer. The assay solutions contained 100 mM buffer, 400 μM $NADP^+$, and varying concentrations of G6P. Assays were initiated by the addition of enzyme and performed in duplicate or triplicate. The $NADP^+$ concentration was chosen to remain saturating at the pH extremes for both enzymes. Concentrations of coenzyme and G6P solutions were determined enzymatically with G6PD.

The apparent k_{cat} and k_{cat}/K_m values obtained at each pH value were determined using the HYPER program of Cleland (*16*), and log k_{cat} or log k_{cat}/K_m values were plotted against pH. The pH profile curves for the wild-type enzyme were similar to those reported by Viola (*15*). The pK_a values were determined using the equations and programs of Cleland (*16, 17*) as described by Viola (*15*). The standard error of

Table 1: X-ray Data Collection Parameters and Statistics

data set	D177N grown with NAD^+	D177N−G6P−NADPH ternary complex	Q365C−G6P complex
space group	C2	C2	C2
cell dimensions			
a =	130.3 Å	129.0 Å	129.8 Å
b =	44.4 Å	44.0 Å	44.3 Å
c =	92.8 Å	91.1 Å	91.2 Å
$\alpha = \gamma$ =	90.0°	90.0°	90.0°
β =	106.7°	105.2°	105.1°
resolution (outer shell)	30−2.54 Å (2.59−2.54 Å)	25−2.3 Å (2.38−2.3 Å) 25−2.48 Å (2.59−2.48 Å)[a]	25−2.69 Å (2.79−2.69 Å)
reflections measured	46 259	47 274 38 083[a]	38 922
unique	15 753	19 062 16 723[a]	13 462
reflections measured once only	1822	39 59 2908[a]	1408
redundancy[b]	3.2	2.9	2.9
$I/(\sigma I)$ (outer shell)	12.7 (3.3)	8.6 (1.7)	9.0 (3.3)
R_{merge} (outer shell)[c]	8.6% (25.9%)	11.5% (51.5%) 10.6% (46.0%)[a]	11.2% (33.1%)
completeness (outer shell)	95.1% (85.6%)	85.3% (36.0%) 93.6% (82.1%)[a]	94.6% (93.1%)

[a] These lines refer to the data set to 2.48 Å resolution with better than 80% completeness in the outer shell. [b] Average number of measurements for each reflection which contributed to the calculation of R_{merge}. [c] $R_{merge} = \sum_{hkl}|\langle I_{hkl}\rangle - I_{hkl}|/\sum_{hkl}\langle I_{hkl}\rangle$, where $\langle I_{hkl}\rangle$ represents the average intensity of symmetry-equivalent reflections.

measurement of the fitted pK_a values are ±0.2 pH units or smaller.

Crystallization. Purified D177N G6PD and Q365C−G6PD[2] were treated similarly for crystallization trials. The enzyme was dialyzed extensively against 0.1 M Tris-HCl pH 7.5 to remove bound coenzyme (D177N) or storage buffer (Q365C). The D177N enzyme was then concentrated to 15 mg/mL using centriflo membrane cones (Amicon) and cocrystallized with 29 mM NAD^+ (neutralized with NaOH) using the hanging drop vapor diffusion technique. The well contained 20% v/v PEG 400 in 0.1 M HEPES−NaOH, pH 7.5, and 0.2 M $CaCl_2$ as described by Naylor (*18*). Crystals appeared after 1 day and were fully grown within 1 week. Initial diffraction studies identified the space group as C2. Similar conditions were used to cocrystallize D177N G6PD with 2.28 mM G6P plus 0.6 mM NADPH with the well containing 14% v/v PEG 400 in 0.1 M HEPES−NaOH, pH 7.5, and 0.2 M $CaCl_2$. Crystals formed after 2 days and were fully grown within 1 week. The space group was again C2.

Q365C G6PD was concentrated to 10 mg/mL and cocrystallized with benzamide adenine dinucleotide (BAD) (*19*) and G6P. The protein drop, 7.5 mg/mL, 10 mM BAD, 20 mM G6P, was equilibrated with well buffer, 21% w/v PEG 400 in 0.1 M HEPES−NaOH, pH 7.8, 0.2 M $CaCl_2$. The space group was again C2.

X-ray Diffraction Data Collection. The two D177N data sets were collected at 100 K in house in Oxford on a conventional source with wavelength 1.5418 Å. Single crystals were soaked briefly in mother liquor containing 15% glycerol and flash frozen in a stream of liquid nitrogen using the Oxford Cryosystems cryostream (*20*). Intensities were recorded on a 30 cm Mar Research image plate. Data were collected to 2.5 Å for D177N G6PD crystals grown in the presence of NAD^+ and to 2.3 Å for D177N G6PD crystals grown in the presence of G6P and NADPH. The data for Q365C−G6PD grown in the presence of BAD^+ and G6P (Q365C−G6P) were collected to 2.7 Å at station 9.6 of the CCLRC Daresbury Laboratory synchrotron source using an X-ray wavelength of 0.88 Å. All data sets were processed using the program suite Denzo (*21*) followed by programs in the CCP4 package (*22*). Cell dimensions and statistics are given in Table 1. Five percent of the terms were set aside for free *R*-factor validation (*23*).

Structure Refinement. Rigid body refinement was carried out for all data sets using the program X-PLOR (*24*) (version 3.851) and the refined coordinates of the isomorphous (C2) S215C apo-enzyme (*18*) as model, omitting bound waters. For the D177N enzyme grown in the presence of NAD^+, initial $2F_{obs} - F_{calc}$ and $F_{obs} - F_{calc}$ electron density maps showed that a low occupancy of NAD^+ was possible in the expected nucleotide-binding region. Further rounds of model building and refinement were carried out using "O" (*25*) followed by energy minimization using X-PLOR. Cycles of simulated annealing were performed in which the coenzyme was omitted to reduce phase bias. The resulting maps were examined, but eventually it was decided that the occupancy of NAD^+ was too low to be modeled successfully. Water molecules were included in the structure where the electron density was at least 1σ in the $2F_{obs} - F_{calc}$ map and at least 3σ in the $F_{obs} - F_{calc}$ map. The final model for the D177N enzyme grown in the presence of NAD^+ contains all 485 G6PD residues, 1 calcium ion, and 68 water molecules and

[2] The mutant Q365C was designed to use for preparing a heavy atom derivative *(13)*. Crystallization experiments indicated that crystals were isomorphous with wild-type enzyme but that they were less susceptible to radiation damage. Residue 365 is on the surface of the enzyme, close to the dimer interface, more than 25 Å from the substrate in either subunit and 40 Å from the coenzyme. Comparison of structures containing glutamine and cysteine at this position shows any changes affect only immediate contacts. The greater stability in the X-ray beam was the main reason for using this mutant in our experiments.

Table 2: Refinement Statistics and Quality Indicators

data set	D177N grown with NAD^+	D177N−G6P−NADPH ternary complex	Q365C−G6P complex
observations in refinement			
working set (outer shell)[a]	14 992 (853)	18 148 (775)[b] 15 926 (1720)[c]	12 817 (1212)
validation set (outer shell)	758 (49)	913 (40)[b] 797 (97)[c]	645 (55)
R-factor (outer shell)	22.2% (38.7%)	21.6% (40.1%)[b] 20.5% (35.3%)[c]	18.0% (26.0%)
free *R*-factor (outer shell)	29.9% (47.9%)	30.9% (58.0%)[b] 29.6% (42.8%)[c]	28.5% (33.2%)
mean *B* main chain atoms	38.2 Å^2	29.1 Å^2	18.8 Å^2
mean *B* side chain atoms	39.6 Å^2	30.4 Å^2	19.7 Å^2
mean *B*-factor for waters	33.4 Å^2	29.8 Å^2	19.2 Å^2
mean coordinate error (Sigmaa)	0.45 Å	0.52 Å	0.27 Å
rmsd distances	0.006 Å	0.006 Å	0.006 Å
rmsd bond angles	1.23°	1.29°	1.25°
rmsd dihedrals	22.3°	22.2°	22.9°
rmsd impropers	0.94°	0.97°	0.92°
Ramachandran plot			
% most favored	88.4	88.8	89.3
% additional allowed	11.4	11.0	10.3
% generously allowed	0	0	0.2
% disallowed (sequence no.)	0.2 (221)	0.2 (221)	0.2 (221)

[a] Resolution limits (outer shell) are, for D177N grown with NAD^+, 30.0−2.54 Å (2.63−2.54 Å) and 25.0−2.69 Å (2.79−2.69 Å) for Q365C−G6P. [b]Resolution limits (outer shell) are, for D177N−G6P−NADPH, 25.0−2.30 Å (2.38−2.30 Å). [c] Resolution limits (outer shell) are, for D177N−G6P−NADPH, 25.0−2.48 Å (2.59−2.48 Å).

is referred to as D177N-nad.[3] The refinement statistics and quality indicators are given in Table 2.

For both the Q365C and the D177N crystals grown in the presence of G6P, the initial $2F_{obs} - F_{calc}$ and $F_{obs} - F_{calc}$ maps showed clearly visible density for the G6P molecule in the cleft between His-178 and His-240. The electron density maps for the D177N−G6P−NADPH complex showed density for at least part of the NADPH molecule in the expected nucleotide-binding site. This data set was refined as described above, using all data to 2.3 Å resolution for much of the refinement, although the data between 2.48 and 2.3 Å were incomplete. Final refinement cycles and electron density maps for this complex have been calculated at 2.48 Å resolution, corresponding to the limit of data with better than 80% completeness. The final model includes 485 G6PD residues, 1 G6P molecule, 1 calcium ion, 131 water molecules and, at 0.75 occupancy, the adenine, 2′-phosphate, adenine ribose, and one phosphate of the bis-phosphate of NADPH. There was only minimal evidence for BAD in the Q365C complex. After refinement, the final model for this complex comprised 485 G6PD residues, 1 G6P molecule, 1 calcium ion, and 108 water molecules. The highest peaks in all final difference electron density maps were less than 1.05 times the rms error level of the ($2F_{obs} - F_{calc}$) maps. Coordinates for the structures of all complexes have been deposited in the Protein Data Bank.[4]

RESULTS AND DISCUSSION

L. mesenteroides G6PD is a homodimer with subunit MW of 54 kD. Each subunit is composed of two domains: a coenzyme binding domain with a classic Rossmann dinucleotide binding fold (residues 1−178), and a large $\beta + \alpha$ domain (residues 179−485) with an antiparallel nine-stranded β-sheet that makes up part of the dimer interface (see Figure 1a of the accompanying paper, ref *26*). The pocket that is formed between domains is lined with conserved residues, including an eight-residue peptide (residues 175−182), and makes up the putative active site (*2*). Site-directed mutagenesis has confirmed the importance of several of these residues in the mechanism of the reaction catalyzed by G6PD (*3*) or, in binding the substrate, G6P (*3*, *12*, *26*). This paper considers the effect on the structure and activity of G6PD of the mutation of Asp-177 to Asn; the structures of the D177N G6PD in the presence and absence of substrate are compared with those of mutants with normal activities. It focuses on the effect on substrate binding and catalysis, comparing the G6P site in the D177N ternary complex with that of a G6P complex of a G6PD mutant with normal activity. Since the reduced nicotinamide nucleotide is disordered in the D177N ternary complex, it contributes little to the substrate-binding site; coenzyme binding will be discussed elsewhere.

The three-dimensional structure of H240N G6PD has previously been solved by X-ray crystallography in the presence of sulfate (*3*). The H240N enzyme displayed no changes in the overall fold of the protein, but changing His-240 to asparagine resulted in a linked movement of active site residues Asp-177 and His-178. The movement of His-178 in the H240N enzyme was correlated with increased Michaelis constants for G6P in both the NAD- and NADP-linked reactions and in an increased K_d for G6P (*3*).

In the present studies, the enzyme was crystallized under different conditions from those for the H240N G6PD structure described above. Both D177N and Q365C enzymes were crystallized with PEG 400 plus $CaCl_2$ as precipitant to avoid the use of phosphate or sulfate ions that in binding to the enzyme may have contributed to earlier failures to bind

[3] D177N-lowercase nad (D177N-nad) is used throughout to represent the model for the D177N mutant enzyme that was crystallized in the presence of NAD^+. Lowercase nad is used to signify that little NAD^+ bound and it was not modeled in the refinement.

[4] Ramachandran plots are included as supplementary data for the use of those who choose to reference them.

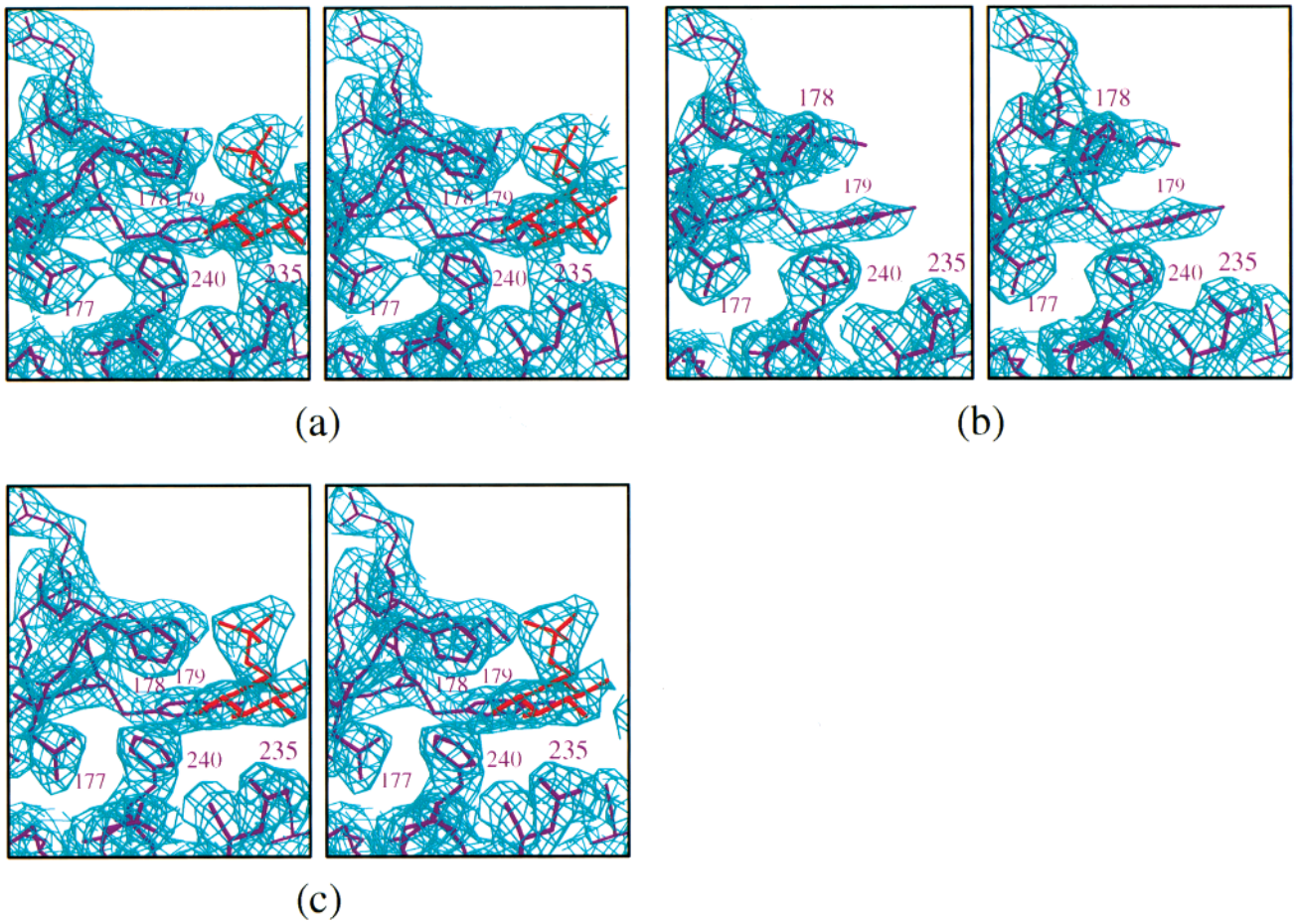

FIGURE 1: Stereoviews of the active site region in (a) the D177N ternary complex, (b) the D177N-nad molecule, and (c) the Q365C−G6P complex. The $2F_{obs} - F_{calc}$ electron density maps are contoured at 1σ, and residues of interest are identified. The bound substrate is highlighted in red. The figure was prepared using BOBSCRIPT (*28*, *29*).

substrate. The new conditions have allowed a range of cocrystallizations with coenzyme, substrate, and analogues to be explored (*18*). These include D177N G6PD with substrate, G6P, and reduced coenzyme, NADPH; D177N G6PD with oxidized coenzyme, NAD^+; and the fully active G6PD mutant, Q365C, with G6P and potential coenzyme inhibitor, BAD. In these crystallization conditions, a calcium ion is frequently bound at a crystal contact between dimers. It is distant from the active site and will not be discussed further.

G6P Binding to G6PD, D177N and Q365C Mutants. The $2F_{obs} - F_{calc}$ electron density maps of the active site regions of the D177N ternary complex, the D177N-nad molecule, and the Q365C−G6P complex are compared in Figure 1. Steady state kinetic analyses of the NADP-linked reaction of the D177N mutant enzyme at pH 7.8 demonstrated a significant decline in k_{cat} with respect to wild-type G6PD with little effect on the Michaelis constants for G6P and $NADP^+$ (*3*). Additionally, the thermodynamic binding constant for G6P is similar to that in wild-type G6PD (*3*). Therefore, it had been anticipated that the positions of the ligands in the D177N−G6P−NADPH ternary complex would be very similar to their positions in the wild-type enzyme.

The details of G6P binding are revealed in the structures of the D177N−G6P−NADPH and Q365C−G6P complexes. Figure 2 shows the hydrogen-bonding network in each substrate binding site. The protein contacts to G6P are all conserved and listed in Table 3. As expected, G6P is bound in the pocket between domains, with hydrogen bonds to both His-178 and His-240.

Phosphate Moiety of G6P. Wild-type G6PD crystallized in the presence of phosphate contains two phosphates in the putative active site of one subunit and one in the other (*2*) and is considered to be an enzyme−phosphate inhibitor complex. The phosphate common to both subunits binds at the Nδ1 position of His-178, suggesting this as the site for the phosphate moiety of G6P. The other phosphate is bound less tightly at the Nϵ2 position of His-178. Site-directed mutagenesis of His-178 had confirmed its importance in binding G6P; the H178N mutant enzyme showed a 400-fold increase in the K_m for G6P, a 10-fold increase in the K_d for G6P, and lost the ability to discriminate effectively between G6P and D-glucose (*3*).

The G6P phosphate moiety, however, is bound at the His-178 Nϵ2 phosphate-binding site and not at the Nδ1 site as expected. Rather, in the D177N ternary complex, a well ordered water molecule (605) is bound to Nδ1 of His-178 (Figure 2). This water makes a second hydrogen bond to the main chain amino group of His-178 and is part of a chain of three, linking back to the carbonyl of Ile-176; the second water (690) is also hydrogen-bonded to His-240 Nϵ2. Water 605 is absent or less well ordered in the Q365C−G6P complex. The difference may result from the presence of bound NADPH in the D177N complex or from the replacement of Asp-177 with asparagine. It may also be that the

Table 3: G6P Ligands

G6P atom	residue number	type	atom	distance Å D177N	distance Å Q365C
O1	240	His	Nϵ2	2.80[a]	2.79[a]
O2	235	Asp	Oδ1	2.66[a]	3.12[a]
O3	235	Asp	Oδ2	3.03[a]	3.47
	223	Arg	Nϵ	>4	3.18[a]
	338	Lys	Nζ	3.18[a]	3.34[b]
O4	216	Glu	Oϵ1	2.82[a]	2.90[a]
O6	178	His	Nϵ2	3.33[b]	3.47
	179	Tyr	Oη	3.67	3.00[a]
O7	698	Wat	O	2.48[a]	
O8	178	His	Nϵ2	2.69[a]	2.72[a]
	182	Lys	Nζ	2.97[a]	3.15[a]
O9	179	Tyr	Oη	2.69[a]	2.92[a]
	182	Lys	Nζ	>4	3.31[b]
	343	Lys	Nζ	2.63[a]	2.79[a]

[a] Indicates potential hydrogen bond (≤3.25 Å). [b] Indicates borderline potential hydrogen bond (<3.35 Å).

different resolutions of the data sets resulted in this water not reaching the 3σ level in the Q365C difference map.

Other protein ligands for the phosphate moiety are Tyr-179 Oη, Lys-182 Nζ of the conserved peptide, and Nζ of Lys-343. Additionally one phosphate oxygen has a water ligand (698), which binds a second water (608), itself bound to Oϵ1 of the conserved Glu-216. Equivalent protein contacts are found in Q365C−G6P, but the waters are not seen.

Sugar Moiety of G6P. Site-directed mutagenesis of His-240 to asparagine resulted in a decrease in k_{cat} by a factor of almost 10^5 for both the NAD- and NADP-linked reactions (*3*). The O1 of G6P is 2.8 Å away from the Nϵ2 atom of His-240 in both the Q365C−G6P and D177N−G6P−NADPH complexes (Table 3). Taken together, these results confirm that the general base of the reactions catalyzed by G6PD is His-240. Asp-235 forms a two-point interaction with the O2 and O3 moieties of G6P in the D177N−G6P−NADPH ternary complex (Figure 2a), and there is also a contact to a water (574). This two-point interaction is not as evident in the Q365C−G6P complex where Asp-235 forms one H-bond with O2 of G6P and another with water 654 (equivalent to 574). The conserved residue Arg-223 is flexible on a mobile loop; it appears to be more important in the Q365C−G6P complex as the major conformation will form a hydrogen bond with O3 of G6P. The interaction is not apparent for the major side chain conformation in the ternary complex, but there is some evidence that it may be present in a minor conformation. Glu-216, at the beginning of the same loop, is conserved and H-bonds with the O4 of G6P. Conserved Lys-338 H-bonds with the O3 of G6P.

Structural Effects of Replacing Asp-177 with Asn. D177N−G6PD Active Site Compared to that of S215C−G6PD. Very few differences are apparent in the overall structure of G6PD when Asp-177 is replaced by Asn. Differences within the active site region are again small for most residues, with the exception of His-178. Superimposed active sites are shown in Figure 3.

Implications of Movement of His-178. The most significant structural differences between the S215C apo-enzyme (*18*) and D177N-nad G6PD are movement of the Cα atom of His-178 by 1.3 Å and rotation of its side chain by almost

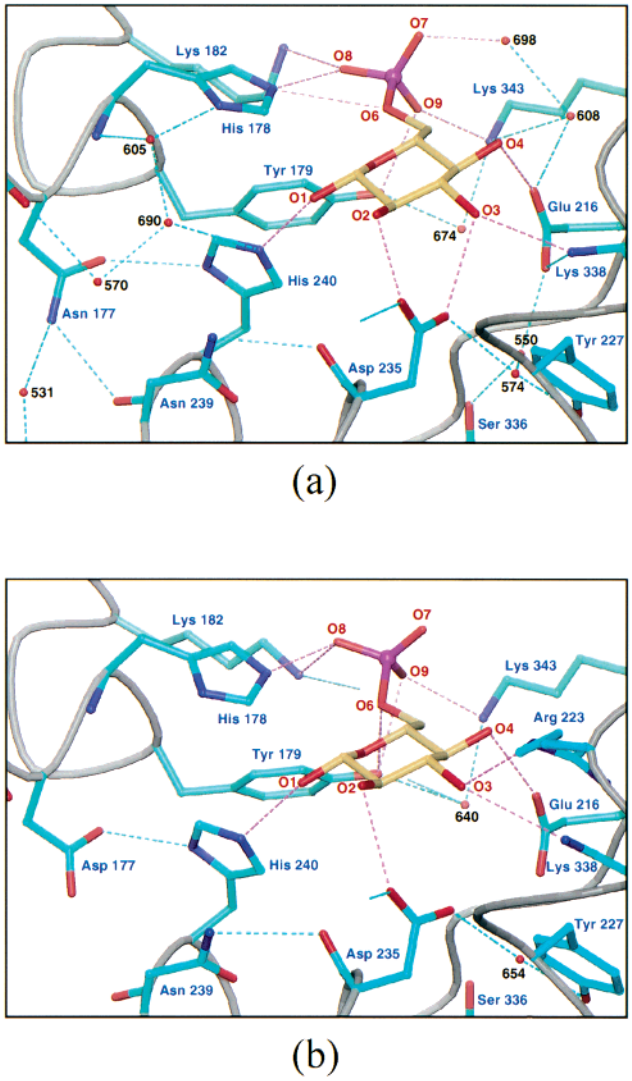

FIGURE 2: Hydrogen-bonding network in the active site regions of (a) the D177N ternary complex and (b) the Q365C−G6P complex. The orientation used is equivalent to that in Figure 1. Potential hydrogen bonds are shown as dotted lines, those which directly involve atoms of the substrate are colored pink, and others are cyan. (Hydrogen bonds are defined as in Table 3. In addition, contacts of 3.25−3.35 Å between protein and G6P are included if the angles are appropriate.) Side chain atoms of the protein are colored according to type with carbon as cyan, oxygen as red, and nitrogen as blue; carbon atoms of the substrate are cream, oxygen atoms are red, and the phosphorus atom is purple. The figure was prepared using BOBSCRIPT (*28, 29*) and RASTER3D (*30, 31*).

180° about the Cα−Cβ bond, resulting in the positions of the Nϵ2 atoms in the two structures being 3.7 Å apart. If the S215C−NAD^+ complex (*18*) is compared with D177N-nad G6PD, the side chain of His-178 is in a third orientation, again with a separation of Nϵ2 atoms of 3.7 Å. There is much smaller difference in Cα positions for these two structures, and the S215C−NAD^+ complex is an intermediate in this respect with an intermediate rotation of the His-178 side chain; the Nϵ2 atom is moved 2.8 Å relative to S215C apo-enzyme. In the absence of substrate, His-178 can adopt several conformations by rotation around the Cα−Cβ bond (Figure 3a). The flexibility is lost in the presence of G6P with His-178 in equivalent positions (Figure 3b), similar to that in the phosphate−inhibitor complex (*2*), in both G6P complexes. This orientation is also found in the S215C apo-

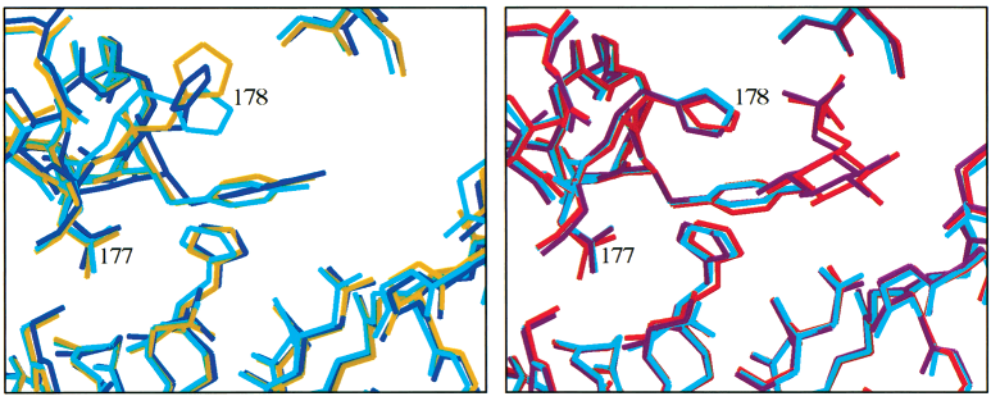

FIGURE 3: Superimposed active site regions for the (a) D177N-nad (blue), S215C apo-enzyme (cyan), and S215C−NAD^+ (gold) and (b) D177N−G6P−NADPH (red), Q365C−G6P (purple), and S215C apo-enzyme (cyan). The figure was prepared using BOBSCRIPT (*28*, *29*).

enzyme where one water is seen corresponding to water 605 of the D177N ternary complex but the water chain does not continue. Although it has been shown that His-178 contributes to the binding energy of the phosphate moiety of G6P (*3*), it is not likely that the differences in the position of His-178 could account for the loss of activity when Asp-177 is replaced by asparagine. In this mutant, His-178 still can reorient to bind G6P and the Michaelis constants for G6P are unaffected in either D177N or S215C G6PDs.

Orientation of Asn-177. Although it is not possible to determine the orientation of the side chain of asparagine from an electron density map, it can sometimes be inferred from the hydrogen-bonding pattern. In D177N-nad G6PD, the side chain of Asn-177 is oriented with one of the terminal atoms of the carboxamide 3.0 Å from the Nδ1 atom of His-240 and the other 3.3 Å from the carbonyl oxygen of Asn-239. In the ternary complex (Figure 2a) these distances are 3.0 and 3.1 Å, respectively. These may be compared with 3.1 and 2.8 Å from His-240 Nδ1 to Asp-177 Oδ1 and with 3.5 and 3.4 Å from Asp-177 Oδ2 to Asn-239 O in the S215C enzyme and the Q365C−G6P complex, respectively. These contacts suggest a hydrogen-bonding pattern such that the carbonyl group of the carboxamide moiety of Asn-177 in the D177N enzyme is oriented toward His-240, and such that the amino group is oriented toward the carbonyl of Asn-239.

Replacement of Asp-177 with asparagine does not significantly affect the position of His-240 in the models for the D177Nand S215C enzymes. This result combined with the hydrogen-bonding pattern described above suggests that the imidazole moiety of His-240 is in the proper tautomeric form for catalysis. Since the imidazole in the D177N enzyme is in a similar orientation to that in S215C G6PD, it follows that the charge of Asp-177 is not necessary for orientation of the imidazole side chain; a hydrogen bond appears sufficient for this purpose.

This contrasts with the results already discussed for rat trypsin and ribonuclease A (*7*, *8*) where the aspartate was seen to be necessary to stabilize the productive tautomer of the histidine. In D177N G6PD, however, the productive tautomer of His-240 is stabilized by virtue of the hydrogen-bonding pattern with Asn-177. This indicates that the loss of activity when Asp-177 is replaced with asparagine is not due to the failure to stabilize the correct tautomer of His-240 but due to the influence of the charge of the functional group of residue 177 on the ionization behavior of His-240. The His-Asp dyad of G6PD is then seen to be similar in this respect to that of mandelate racemase where replacement of Asp-270 with asparagine resulted in only a slight perturbation of the imidazole ring of the catalytic His-297 (*9*).

D177N G6PD Compared to Q365C G6PD and S215C G6PD. The three-dimensional structure of the D177N−G6P−NADPH ternary complex has been compared with that of the Q365C−G6P complex and that of the S215C apo-enzyme. The overall main chain rms deviations between models are 0.30 and 0.24 Å. The fit is worse when the D177N-nad structure is compared to the D177N−G6P−NADPH and Q365C−G6P complexes (rmsds 0.41 and 0.52 Å, respectively), indicating the possibility of an overall main chain conformation change when G6P binds to D177N G6PD.

The fit between the individual domains of D177N-nad and the D177N−G6P−NADPH ternary complex is closer than that of the whole molecule. This comparison results in rms deviations of 0.27 and 0.28 Å for the small and large domains, respectively. This suggests a small difference in the overall relationship between domains: superpositions indicate a slightly more open active site cleft for D177N when G6P is not bound; the differences are on the borderline of significance. The difference in hinge angle may correlate with the different orientations of the side chain of His-178. It may be significant that the unit cell volumes are smaller for the D177N−G6P−NADPH ternary complex and Q365C−G6P binary complex than for D177N-nad G6PD (Table 1).

pH Dependence of Kinetic Parameters. To better understand the effect of Asp-177 on the ionization properties of His-240, the pH dependence of kinetic parameters has been determined for D177N G6PD and compared to that for wild-type G6PD. Figures 4 and 5 show log−log plots of the dependence of k_{cat} and k_{cat}/K_m on pH for both D177N and wild-type G6PDs, respectively.

The Dependence of k_{cat} on pH. The dependence of k_{cat} and k_{cat}/K_m on pH for the NADP-linked reaction of *L. mesenteroides* G6PD was first reported by Viola (*15*). With G6P as the varied substrate, the dependence of k_{cat} on pH was described by two pK_a values at pH 6.3 and 8.7. Protonation of these residues results in enzyme forms with

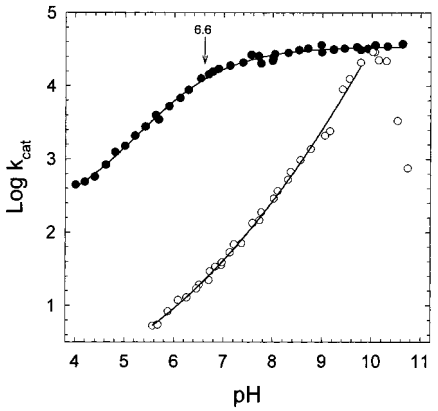

FIGURE 4: Dependence of k_{cat} on pH for wild-type (●) and D177N (○) G6PDs. The log k_{cat} values were plotted against pH, and the wild-type data were fit to the equation: log k_{cat} = log((LO + HI(K_a/[H^+]))/(1 + K_a/[H^+])), where LO and HI are the k_{cat} values of the low and high pH enzyme forms, [H^+] is the proton concentration, and K_a is the dissociation constant for an acidic group. The arrow indicates the position of the pK_a value derived from the fit. The best fit to the data derived from assays of the D177N enzyme between pH 5 and 10 was obtained with a quadratic equation and nonlinear least-squares regression analysis. The data above pH 10 were not fit (see discussion in text).

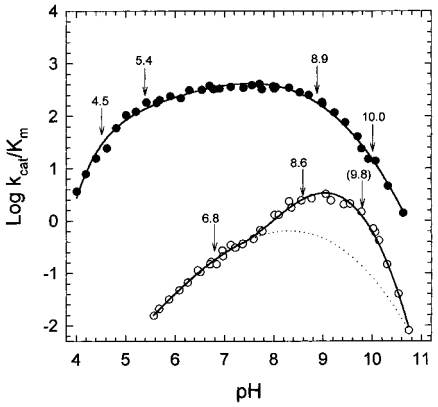

FIGURE 5: Dependence of k_{cat}/K_m on pH for wild-type (●) and D177N (○) G6PDs. Log k_{cat}/K_m values were plotted against pH, and wild-type data were fitted to the equation: log k_{cat} = log(C/(1 + [H^+]/K_1 + [H^+]^2/K_1/K_2 + K_3/[H^+] + K_3K_4/[H^+]^2), where C is the theoretical maximal k_{cat}/K_m with all groups in their preferred ionization state, [H^+] is the proton concentration, and K_1, K_2 and K_3, K_4 are the dissociation constants for the two acidic and two basic groups, respectively. The k_{cat}/K_m data derived from the D177N enzyme were fit to eq 1 as described in the text. The value in parentheses (9.8) indicates an apparent pK_a for the reasons described in the text. The dotted line indicates the expected pH profile for D177N G6PD in the absence of OH^- dependence, using the value of k_{enz} reported in the text, pK_a values of 6.8, 8.9, and 10.0, and a modified form of the above equation to account for the dissociation of one acidic and two basic groups. Arrows indicate positions of pK_a values derived from the fits.

reduced activity. It was suggested that the pK_a of 6.3 was associated with a change in the overall charge of the protein, while the pK_a of 8.7 was assigned to a step in the mechanism associated with product release. This experiment was repeated in this investigation with recombinant wild-type *L. mesenteroides* G6PD. The results are qualitatively similar to those reported by Viola (*15*) with the exception that the pK_a at 8.7 was not evident from the log−log plot. The best fit to the data was obtained by assuming that the ionization of one group causes loss of activity in the enzyme−substrate complex with a pK_a value of 6.6. Changing Asp-177 to asparagine results in a 100-fold decline in k_{cat} for both the NAD- and NADP-linked reactions at pH 7.8 (*3*), but the D177N mutant enzyme regains full activity at high pH (Figure 4). Since the activity of D177N G6PD at pH 7.8 is unaffected by preincubation at high pH (data not shown), asparagine deamidation can be ruled out as the cause for this regain of activity.

The k_{cat} profile for D177N G6PD shows a nearly linear increase from pH 5 until wild-type-like activity is regained at pH 10. Above pH 10 the k_{cat} decreases precipitously (see below). Linear regression of the data in the pH range 5−10 produces a slope of 0.9 ± 0.02, however, with a nonrandom distribution of residuals indicating the model is more complex. A better fit is obtained with a quadratic equation assuming that the k_{cat} dependence below pH 7.5 is due to enzymatic catalysis by the D177N enzyme, and the nearly linear dependence between pH 7.5 and 10 is due to the participation of a titratable base or of a hydroxide ion. The three-dimensional structure of the D177N−G6P−NADPH ternary complex supports the latter, in that there is a well-bound water molecule (690) that is 3.2 Å from the Nϵ2 position of His-240 (Figure 2a). This water molecule is hydrogen-bonded to water 605, which is bound to the Nδ1 position of His-178 and is 3.8 Å from the imidazole ring of His-240. It is unlikely that specific base catalysis is the cause of the linear dependence of k_{cat} on pH in the D177N enzyme because this behavior was not observed in a similar experiment with the H240N enzyme (data not shown).

These observations suggest the following model: as the hydroxide ion concentration increases with increasing pH, the well-bound water molecule ionizes and introduces a localized negative charge next to His-240, replacing the charge of the aspartate in D177N G6PD and leading to full recovery of activity at high pH. In wild-type enzyme, this water molecule may be present and facilitate catalysis by helping to regenerate the conjugate base form of His-240 after oxidation of G6P. If these hypotheses are correct, we would expect that removing His-178 of the wild-type enzyme would remove the binding site for this water molecule and have a significant effect on k_{cat}. Site-directed mutagenesis of His-178 to asparagine not only resulted in impaired ability of the enzyme to bind G6P but also resulted in an order of magnitude decrease in k_{cat} for both the NAD- and NADP-linked reactions at pH 7.8 (*3*).

This model can be invoked to explain the decrease in k_{cat} above pH 10 in that deprotonation of residues important for binding the phosphate moiety of G6P results in the inability of the enzyme to bind G6P and order His-178, which is necessary to form the water binding site. Consistent with this, the three-dimensional structures of the G6PDs described in this paper suggest that this water binding site requires the binding of G6P to order and orient His-178 (Figure 3). Additionally, G6P Michaelis constants are increased at high pH for the D177N enzyme compared to that for the wild-type enzyme (data not shown). It is likely that the reason this loss of activity is not observed in the wild-type enzyme is that the presence of the charged functional group of Asp-177 does not depend on the orientation of His-178, whereas the binding of the water that replaces the negative charge at high pH in the D177N enzyme does depend on the orientation of His-178.

The Dependence of k_{cat}/K_m on pH. The dependence of log k_{cat}/K_m on pH for wild-type G6PD is bell-shaped with limiting slopes of 2 and −2, suggesting the presence of four ionizable groups (*15*). At low pH, an amino acid residue with a pK_a of 4.5 was assigned as the general base of the reaction, and because of the behavior in response to changes in solvent composition, the author attributed it to a neutral acid such as a carboxylate-containing amino acid (*15*). The other pK_a on the acidic side of the profile (5.5) was assigned to the phosphate of G6P. At high pH, the two pK_a values at 9.3 and 10.3 were assigned to amino acids that are ligands to the phosphate moiety of G6P. In this investigation, the results with recombinant wild-type *L. mesenteroides* G6PD were both qualitatively and quantitatively similar with fitted pK_a values of 4.5, 5.4, 8.9, and 10.0 (Figure 5).

When Asp-177 is replaced with asparagine, the k_{cat}/K_m pH profile becomes more complex, with a narrow range of maximal activity extending from about pH 8.5 to 9.6 and a shoulder that extends from pH 6.6 to 7.5 (Figure 5). The basic limb of the k_{cat}/K_m profile (pH 9−11), like that for the wild-type enzyme, appears to have a limiting slope of −2, suggesting the involvement of two ionizing groups. The fit to this model, however, produces two pK_a values that are too close to be distinguished at 9.6 ± 0.12 with a nonrandom distribution of residuals. Repeating the fit with fewer points produced a better fit with two pK_a values at 9.8 ± 0.07; however, the residuals were still not randomly distributed. This suggests that the profile is falling more steeply than expected for just two pK_a values. However, given the drop in k_{cat} above pH 10 (Figure 4), it is likely that this steepness in the k_{cat}/K_m profile is due to perturbation by some other factor, such as the involvement of hydroxide ionization as described in the previous section (see also discussion below) or enzyme instability at high pH. It should be noted that all rates measured at high pH were linear (data not shown), decreasing the likelihood that the latter accounts for this perturbation.

The rest of the D177N k_{cat}/K_m profile (pH 5−9) was very similar to that observed for the D102N mutant of trypsin (*27*), which fit best to a bipartite rate equation where one part describes the enzyme-catalyzed rate at the lower pH values and the other part shows the catalytic rate that depends on hydroxide ion concentration (*27*):

$$\log(k_{cat}/K_m) = \log\left[\left(\frac{k_{enz}}{1 + [H^+]/K_a + K_b/[H^+]}\right) + \left(\frac{k_{OH}[OH^-]}{1 + (K_b/[H^+])}\right)\right] \quad (1)$$

where k_{enz} is the rate constant of the hydroxide-independent pathway, K_a and K_b are the dissociation constants of the ionizing groups, and k_{OH} is the rate constant of the hydroxide ion-dependent pathway.

Applying this model to the acidic limb of the pH profile for D177N G6PD, we find that values of k_{cat}/K_m above pH 7.5 show an increase with solvent hydroxide ion concentration that yields k_{OH} and K_b values of 1.44 ± 0.17 × 10^6 M^{-2} min^{-1} and 2.5 ± 0.63 × 10^{-9} M (pK_a = 8.6), respectively. It is likely that the pK_a at 8.6, and the apparent pK_a at 9.8, corresponds to groups that ionize at pH 8.9 and 10.0 in the wild-type enzyme, respectively (Figure 5). Probable assignments for these ionizations include Lys-182 and Lys-343, which have been shown by site-directed mutagenesis (*26*) and X-ray crystallography (see Figure 2) to be important for binding the phosphate moiety of G6P.

Measurement of k_{cat}/K_m values below pH 7.5 yields k_{enz} and K_a values of 0.89 ± 0.08 M^{-1} min^{-1} and 1.6 ± 0.3 × 10^{-7} M (pK_a = 6.8), respectively. This pK_a at 6.8 may represent the acid dissociation constant of the general base of the reaction, His-240, in the D177N enzyme. Why this pK_a is not observed in the k_{cat}/K_m profile of the wild-type enzyme is an important question that deserves further study.

A comparison of the k_{enz} value for D177N G6PD and the maximal k_{cat}/K_m value (pH ∼ 7.8) for wild-type G6PD indicates that the presence of aspartate at position 177 increases the rate of the reaction by ∼450-fold. Since replacement of Asp-177 with asparagine does not affect the orientation or the tautomeric form of His-240, this rate enhancement must be due to the effect of the negative charge of Asp-177 on the pK_a of the general base His-240. Determining precisely how this occurs will improve our understanding of the reaction catalyzed by G6PD, as well as advance our general understanding of the role of aspartate in the His-Asp catalytic dyad.

CONCLUSION

In this investigation, we sought to establish the role of Asp-177 in the catalytic mechanism of G6PD from *L. mesenteroides*. It has been proposed that the function of aspartate residues in His-Asp dyads is to stabilize the productive tautomer of the catalytic histidine, to alter its pK_a, and/or to optimally orient histidine for catalysis (*7*−*9*, *27*). We have determined the X-ray structures of the D177N mutant G6PD in the presence of NAD^+ and in the presence of G6P plus NADPH, and we have determined the X-ray structure of the G6P complex of the active mutant Q365C. We have thereby established the contacts involved in binding substrate to the enzyme. The results indicate that removal of the charge supplied by Asp-177 is sufficient to account for the loss of activity of D177N G6PD at pH 7.8. Additionally, the hydrogen-bonding pattern among His-240, Asn-177, and Asn-239 suggests the orientation of the amide of Asn-177 and that the active tautomer of His-240 is stabilized. Variation of the pH dependence of kinetic parameters has shown significant differences from wild-type G6PD and suggests a mechanism where a well-bound water molecule replaces the charge of Asp-177 in D177N at high pH. His-178 appears to play an important role in forming the binding site for this water molecule. The conclusions presented here suggest that like mandelate racemase *(9)*, the function of the Asp in the His-Asp catalytic dyad of G6PD is to affect the pK_a of the histidine, enhancing its ability to abstract the proton from the substrate. Since this was not observed with trypsin *(7)* or ribonuclease A *(8)*, despite the use of similar methods, it appears that the role of the aspartate in the His-Asp catalytic dyad in enhancing catalysis may be different in different enzymes.

ACKNOWLEDGMENT

We gratefully acknowledge technical assistance from Valarie E. Vought. We thank Dr. W. W. Cleland for helpful discussions and for his assistance in fitting the kinetic data. We thank Dr. Barry Goldstein for BAD. We thank Dr.

Minakshi Ghosh and Dr. Shannon W. N. Au for helpful discussions. We thank Prof. Louise N. Johnson for facilities and support. M.J.A. is the Dorothy Hodgkin−E. P. Abraham Fellow of Somerville College, Oxford, and an associate member of the Oxford Centre for Molecular Sciences.

REFERENCES

1. Lee, W. T., Flynn, T. G., Lyons, C., and Levy, H. R. (1991) *J. Biol. Chem. 266*, 13028−13034.
2. Rowland, P., Basak, A. K., Gover, S., Levy, H. R., and Adams, M. J. (1994) *Structure 2*, 1073−1087.
3. Cosgrove, M. S., Naylor, C., Paludan, S., Adams, M. J., and Levy, H. R. (1998) *Biochemistry 37*, 2759−2767.
4. Kim, Y. S., Yong, I. K., and Byun, H. S. (1988) *Biochem. Int. 17*, 1099−1106.
5. Haghighi, B., and Levy, H. R. (1982) *Biochemistry 21*, 6429−6434.
6. Domschke, W., Engel, H. J., and Domagk, G. F. (1969) *Hoppe-Seyler's Z. Physiol. Chem. 350*, 1117−1120.
7. Sprang, S., Standing, T., Fletterick, R. J., Stroud, R. M., Finer-Moore, J., Xuong, N.-H., Hamlin, R., Rutter, W. J., and Craik, C. S. (1987) *Science 237*, 905−909.
8. Schultz., L. W., Quirk, D. J., and Raines, R. T. (1998) *Biochemistry 37*, 8886−8898.
9. Schafer, S. L., Barrett, W. C., Kallarakal, A. T., Mitra, B., Kozarich, J. W., and Gerlt, J. A. (1996) *Biochemistry 35*, 5662−5669.
10. Sambrook, J., Fritsch, E. F., and Maniatis, T. (1989) *Molecular Cloning: A Laboratory Manual* 2nd. ed., Cold Spring Harbor Laboratory Press, Cold Spring Harbor, New York.
11. Levy, H. R., Vought, V. E., Yin, X., and Adams, M. J. (1996) *Arch. Biochem. Biophys. 326*, 145−151.
12. Lee, W. T., and Levy, H. R. (1992) *Protein Sci. 1*, 329−334.
13. Adams, M. J., Basak, A. K., Gover, S., Rowland, P., and Levy, H. R. (1993) *Protein Sci. 2*, 859−862.
14. Olive, C., and Levy, H. R. (1971) *J. Biol. Chem. 246*, 2043−2046.
15. Viola, R. E. (1984) *Arch. Biochem. Biophys. 228*, 415−424.
16. Cleland, W. W. (1979) *Methods Enzymol. 63*, 103−135.
17. Cleland, W. W. (1977) *Adv. Enzymol. 45*, 427.
18. Naylor, C. E. (1997) D.Phil. Thesis, Oxford University, Oxford, U.K.
19. Zatorski, A., Watanabe, K. A., Carr, S. F., Goldstein, B. M., and Pankiewicz, K. W. (1996) *J. Med. Chem. 39*, 2422−2426.
20. Garman, E. F., and Schneider, T. R. (1997) *J. Appl. Crystallogr. 30*, 211−237.
21. Otwinowski, Z. (1993) in *Proceedings of the CCP4 Study Weekend*, pp 56−62, SERC, Daresbury Laboratory, Warrington, U.K.
22. CCP 4. (1994) *Acta Crystallogr. D50*, 760−763.
23. Brunger, A. T. (1992) *Nature 355*, 472−474.
24. Brunger, A. T. (1992) *X-plor. Version 3.1. A System for X-ray Crystallography and NMR*, Yale University Press, New Haven, CT.
25. Jones, T. A., Zou, J.-Y., and Cowan, S. W. (1991) *Acta Crystallogr. A47*, 110−119.
26. Vought, V., Ciccone, T., Davino, M. H., Fairbairn, L., Lin, Y., Cosgrove, M. S., Adams, M. J., and Levy, H. R. (2000) *Biochemistry 39*, 15012−15021.
27. Craik, C. S., Roczniak, S., Largman, C., and Rutter, W. J. (1987) *Science 237*, 909−913.
28. Esnouf, R. M. (1997) *J. Mol. Graphics 15*, 132−134.
29. Kraulis, P. J. (1991) *J. Appl. Crystallogr. 24*, 946−950.
30. Merritt, M. A., and Murphy, M. E. P. (1994) *Acta Crystallogr. D50*, 869−873.
31. Bacon, D. J., and Anderson, W. F. (1988) *J. Mol. Graphics 6*, 219−220.

BI0014608